4616–4629 *Nucleic Acids Research, 2022, Vol. 50, No. 8* *Published online 14 April 2022*
https://doi.org/10.1093/nar/gkac229

Programmable cleavage of linear double-stranded DNA by combined action of Argonaute CbAgo from *Clostridium butyricum* and nuclease deficient RecBC helicase from *E. coli*

Rita Vaiskunaite, Jogirdas Vainauskas, Janna J.L. Morris, Vladimir Potapov and Jurate Bitinaite*

Research Department, New England Biolabs, Ipswich, MA 01938, USA

Received August 11, 2021; Revised March 18, 2022; Editorial Decision March 22, 2022; Accepted March 24, 2022

ABSTRACT

Prokaryotic Argonautes (pAgos) use small nucleic acids as specificity guides to cleave single-stranded DNA at complementary sequences. DNA targeting function of pAgos creates attractive opportunities for DNA manipulations that require programmable DNA cleavage. Currently, the use of mesophilic pAgos as programmable endonucleases is hampered by their limited action on double-stranded DNA (dsDNA). We demonstrate here that efficient cleavage of linear dsDNA by mesophilic Argonaute CbAgo from *Clostridium butyricum* can be activated *in vitro* via the DNA strand unwinding activity of nuclease deficient mutant of RecBC DNA helicase from *Escherichia coli* (referred to as RecB^{exo-}C). Properties of CbAgo and characteristics of simultaneous cleavage of DNA strands in concurrence with DNA strand unwinding by RecB^{exo-}C were thoroughly explored using 0.03–25 kb dsDNAs. When combined with RecB^{exo-}C, CbAgo could cleave targets located 11–12.5 kb from the ends of linear dsDNA at 37°C. Our study demonstrates that CbAgo with RecB^{exo-}C can be programmed to generate DNA fragments with custom-designed single-stranded overhangs suitable for ligation with compatible DNA fragments. The combination of CbAgo and RecB^{exo-}C represents the most efficient mesophilic DNA-guided DNA-cleaving programmable endonuclease for *in vitro* use in diagnostic and synthetic biology methods that require sequence-specific nicking/cleavage of linear dsDNA at any desired location.

INTRODUCTION

Eukaryotic Argonautes (eAgo) are essential components of the RNA-induced gene silencing processes (1,2). The mechanism involves the association of eAgo with a single-stranded RNA guide to form an RNA-induced silencing complex (RISC) (3,4). The RISC is directed to the complementary sequence on mRNA where the Argonaute cleaves single-stranded mRNA in a guide specific manner resulting in reduced target gene expression (5–7). RISC can also interact with various Argonaute-associated proteins to induce cleavage-independent mechanisms of gene regulation (8,9). Prokaryotes lack RNA interference pathways; however, many bacteria and archaea possess Argonaute proteins implying a different biological role for these proteins (10). Multiple recent studies suggest that prokaryotic Argonautes (pAgos) function *in vivo* as defense systems against foreign genetic elements (10–14). pAgos represent a very diverse group of proteins and the presence of four common domains (N, PAZ, MID and PIWI) divides them into two major groups: the short pAgos and the long pAgos (10,12,15). Short pAgos lack the N and PAZ domains. Long pAgos, like eAgos, contain all four common domains and encompass all known active pAgos (12,15,16). In contrast to eAgos, which exclusively use RNA guides to target RNA, bacterial Agos have been shown to bind either RNA or DNA guides and cleave either RNA or DNA targets (17–20). Some archaeal Agos exclusively utilize DNA guides for cleavage of DNA targets (21,22).

Many pAgos exhibit a non-specific nuclease activity when they are not associated with guides (23–25). The nuclease activity of a guide-free pAgo was implicated in cellular function required for guide processing (23). TtAgo co-purifies with DNA sequences preferentially derived from its own expression plasmid, but only if the Argonaute is

*To whom correspondence should be addressed. Tel: +1 978 927 5054; Fax: +1 978 921 1350; Email: bitinaite@neb.com
Present addresses:
Jogirdas Vainauskas, Department of Chemistry, McGill University, Montreal, Quebec H3A 0B8, Canada.
Janna J.L. Morris, Ultragenyx Pharmaceuticals, Cambridge, MA 02139, USA.

catalytically active (26). The recent study of mesophilic bacterial Argonaute CbAgo from *Clostridium butyricum* shows CbAgo nucleolytic activity cooperates with the cellular double-strand break repair machinery in the generation of small DNAs (smDNAs) that can later be used as guides by this Argonaute (14). Chromosomal mapping of CbAgo-bound smDNAs revealed that they are distributed throughout the whole genome with the elevated levels mapped to the sites of double-stranded breaks, the site of replication termination and the specific regions of multicopy genetic elements (14). Similar studies were also carried out with the SeAgo Argonaute from *Synechococcus elongatus* and with the KmAgo Argonaute from *Kurthia massiliensis* (27,28). SeAgo showed preferences for chromosomal regions associated with the sites of replication initiation and replication termination, whereas the KmAgo-bound smDNAs were enriched around the region of replication origin and the DE3 prophage insertion site. Altogether, these studies imply that *in vivo* Ago nucleases actively participate in various genetic processes that involve partial melting of DNA duplex, such as DNA repair, DNA replication, or diverse incidents of chromosome rearrangements (14,27,28).

The ability to direct DNA guides for cleavage of complementary DNA targets opens an opportunity for using pAgos as programmable DNA endonucleases (29). So far, the CRISPR-Cas9 system is the most widely used enzymatic tool for programmable DNA cleavage. Cas9 nuclease programmed with RNA guide can invade double-stranded DNA and generate double-strand breaks at a guide-specific location (30,31). The CRISPR-Cas9 systems function at physiological temperatures, so they have been successfully adapted for genome editing *in vivo* (reviewed in 32). In contrast to CRISPR-Cas9, the cleavage of double-stranded targets by pAgos can only proceed if DNA strands are separated beforehand. Argonaute from the archaeon *Pyrococcus furiosus* (PfAgo) was shown to work as a programmable DNA-guided DNA-cleaving endonuclease *in vitro*, but only because PfAgo is active at a temperature (>87°C) causing thermal DNA denaturation (33). After DNA melting takes place, the double-strand cleavage by PfAgo still proceeds by way of two independent strand-nicking events catalyzed by two PfAgo monomers loaded with separate guides that are complementary to the opposing DNA strands (33). The characterized pAgos functioning at lower temperature range (30–75°C) *in vitro* show greatly reduced endonucleolytic activity on dsDNA compared to ssDNA, and preferentially cleave negatively supercoiled plasmids and DNA sections with low G/C content consistent with the greater single-stranded character of these substrates (25–28,33–37).

Bioinformatics analysis of pAgo operons reveals the abundance of genes encoding diverse range of putative nucleases, helicases, and DNA-binding proteins (10,15,38). Their possible connection remains unclear, but if pAgos are involved in chopping foreign dsDNA then they very likely collaborate with other cellular proteins that can open the DNA duplex. Such theoretical speculation gained some experimental support in the case of thermophilic Argonaute from *Thermus thermophilus* (TtAgo) which showed an elevated activity on dsDNA when cleavage was carried out in the presence of single-strand binding protein ET SSB or TthUvrD DNA helicase (34). Double-stranded DNA cleavage by the mesophilic Argonaute from cyanobacterium *Synechococcus elongatus* (SeAgo) was tested *in vitro* during ongoing transcription of a target region which was expected to transiently melt dsDNA, but the approach had little effect on target cleavage (27).

DNA helicases represent a large and diverse group of proteins involved in various biologically essential cellular processes (39). Most DNA helicases require either a 5′- or 3′-single-stranded DNA (ssDNA) end as an initiation point to start unwinding DNA duplex and typically do not bind to blunt-ended dsDNA. One exception is *Escherichia coli* RecBCD DNA helicase that prefers unwinding blunt-ended DNA and is inhibited by ssDNA ends that exceed ∼25 nucleotides (40). The native RecBCD (also referred as Exonuclease V) cannot unwind circular duplex DNA molecules, whether they are supercoiled, relaxed, or gapped circles, indicating that free ends are essential for helicase activity (40,41). The RecBCD enzyme remains the fastest (1000–2000 bp s^{-1}) and most processive (∼30 000 bp) helicase reported in the literature (42). Wild type RecBCD is a heterotrimer consisting of three subunits, RecB, RecC and RecD. It has multiple enzymatic activities: ATP-dependent DNA unwinding activity, ATP-dependent dsDNA and ssDNA exonuclease activity, ATP-stimulated ssDNA exonuclease activity and ATPase activity (42,43). The RecB subunit is organized into a 100-kDa N-terminal helicase domain and 30-kDa C-terminal exonuclease/endonuclease domain (44). The C-terminal domain of the RecB subunit is responsible for all nuclease activities associated with the RecBCD complex (45,46). The crystal structure of the RecBCD enzyme reveals four conserved catalytic residues (Glu1020, Asp1067, Asp1080 and Lys1082) in the active site of the RecB nuclease domain (47). Nuclease activity of the RecBCD enzyme can be inactivated completely by mutation of either aspartate residue to alanine or lysine residue to glutamine (46). The RecBC enzyme also possesses DNA unwinding activity *in vitro* and in *vivo*, however, it is a slower and less processive helicase than the RecBCD enzyme (48,49). Nevertheless, the RecBC helicase was shown to unwind 21.4 kb linear dsDNA in the matter of minutes (50).

In the present study, we report that mesophilic Argonaute can cleave dsDNA during concurrent unwinding of DNA strands by the nuclease deficient mutant of RecBC DNA helicase referred here as $RecB^{exo-}C$. In total, we screened 20 putative pAgos for cleavage activity at 37–65°C and found ten candidates that were active at 37°C. Six mesophilic Argonautes originating from *Clostridia* class bacteria were further biochemically characterized. While our studies were underway several other reports were published describing the characterization of mesophilic Argonautes, including CbAgo from *Clostridium butyricum*, CpAgo from *Clostridium perfringens* and IbAgo from *Intestinibacter bartlettii* (25,35–36,51). In our study, the most active Argonaute, CbAgo was paired with the $RecB^{exo-}C$ helicase to synchronize DNA duplex unwinding with the guided cleavage of individual DNA strands at 37°C. A detailed analysis of dsDNA cleavage by CbAgo was carried out using high-throughput capillary gel electrophoresis (34,52). We demonstrate that in the presence of the $RecB^{exo-}C$ helicase, CbAgo efficiently cleaves linear dsDNA ranging from 30 bp

to 25 kb in length and produces DNA fragments flanked with unique single-stranded overhangs that can be ligated to other DNA fragments with complementary overhangs. Currently, a combination of CbAgo and RecB^{exo-}C represents the most efficient DNA-guided DNA-cleaving programmable endonuclease, which can be used *in vitro* for the development of new diagnostic and synthetic biology tools requiring custom-designed nicking/cleavage of linear dsDNA at mesophilic temperatures.

MATERIALS AND METHODS

Bioinformatics analysis for identifying mesophilic pAgos

Candidate Argonaute proteins were identified in a series of steps. Firstly, three known Argonaute proteins, TtAgo (UniProt ID Q746M7), NgAgo (UniProt ID L0AJX6) and PfAgo (UniProt ID Q8U3D2) were aligned using MUSCLE multiple sequence alignment software (53). The resulting multiple sequence alignment was used as an input to PSI-BLAST to search against the UniProt database. The expected threshold was set at 1×10^{-4}, and PSI-BLAST ran multiple iterations until convergence. All bacterial homolog hits were extracted based on taxonomic classification. Only proteins containing PAZ and PIWI domains were considered for further analysis. The presence of catalytic PIWI and PAZ domains in homologs was checked by running HMM search using domain profiles available in the PFAM database (PFAM PF02171 and PF02170 for PIWI and PAZ domain, respectively). The PAZ domain profile in PFAM is built mainly on sequences of eukaryotic proteins and resulted in very few hits when run against bacterial proteins. Therefore, the HMM profile for the bacterial PAZ domain was generated from scratch using HMMER software (54) based on sequences of known Argonaute proteins. Proteins originating from known thermophilic organisms were discarded. Additionally, only proteins that share <90% sequence identity were selected for further analysis. Finally, proteins that did not contain aspartates at conserved PIWI catalytic sites were excluded. The remaining list of 45 bacterial Argonautes is available in Supplementary Table S1.

Constructs for pAgo expression and purification

The codon-optimized genes encoding Argonaute proteins were ordered in pET29a expression vectors from GenScript (Piscataway, NJ, USA). Analytical amounts of 20 Argonaute proteins were synthesized from pET29a plasmids using a PURExpress In Vitro Protein Synthesis kit (New England Biolabs, Inc., Ipswich, MA, USA). The solubility of *in vitro* expressed Ago proteins was verified by the SDS-PAGE analysis. For large-scale expression and purification of CbAgo, CpAgo, IbAgo, CdAgo, CsAgo and CaAgo, the respective genes were subcloned into the pET28c expression vector in frame with the N-terminal 6xHis tag. Argonaute protein expression and purification procedures are provided in Supplementary Methods.

Construction of RecB^{exo-} and RecC expression clones

The nuclease deficient mutant of the RecB DNA helicase referred to as RecB^{exo-}, was constructed by replacing catalytic residues E1020, D1080 and K1082 with alanine residues. A plasmid encoding Exonuclease V (RecBCD) (New England Biolabs, Inc., Ipswich, MA, USA) was used as a template to amplify the recB gene as three overlapping PCR fragments B1 (3080 bp), B2 (200 bp) and B3 (340 bp). Primer sequences can be found in Supplementary Table S3. To introduce the E1020A mutation, the GAG codon was replaced by the GCG codon in the overlapping primers used to amplify fragments B1 and B2. Similarly, to introduce D1080A and K1082A mutations, the codon GAC was changed to GCC and the codon AAA was changed to GCA in the overlapping primers for amplification of fragments B2 and B3. Three recB fragments were directly assembled into a pET28c vector in frame with the N-terminal 6xHis tag employing NEBuilder HiFi DNA Assembly Cloning Kit (New England Biolabs, Inc., Ipswich, MA, USA). Wild type RecC encoding gene was individually sub-cloned into a pET28c vector in frame with the N-terminal 6xHis tag. RecB^{exo-} and RecC protein expression and purification protocols are provided in Supplementary Methods.

Argonaute cleavage assays on single-stranded DNA or RNA substrates

All 5′-FAM labeled substrate oligonucleotides (DNA or RNA) and 5′-phosphorylated guides were purchased from Integrated DNA Technologies (Coralville, Iowa, USA). Nucleotide sequences can be found in Supplementary Table S3. To test the activity of *in vitro* expressed pAgo proteins, a 1 μl of PURExpress sample was mixed with 250 nM guide G-1 (17 nt) in buffer containing 20 mM Bis–Tris propane, pH 8.0, 50 mM NaCl, 2 mM $MgCl_2$, 0.1% (v/v) Triton X-100 and incubated for 20 min at 37°C to form a pAgo/guide complex. The pAgo/G-1 complex was then combined with 50 nM 5′-FAM labeled target T-1 in a 20 μl reaction and incubated for 1 h at 37°C or at 65°C. The reactions were terminated by adding 20 μl stop buffer (95% formamide, 0.025% bromophenol blue, 0.025% xylene cyanol, 5 mM EDTA) and heating the samples for 5 min at 95°C. The cleavage products were separated by gel electrophoresis on 15% denaturing polyacrylamide gel containing 7.5 M urea and 24% formamide and visualized using a Typhoon 9400 Scanner (GE Healthcare Chicago, IL, USA).

Activity assays performed with purified Argonaute proteins were carried out with a 17 nt long guide G-2 (DNA) and G-3 (RNA). For guide loading, 125 nM Ago was combined with 125 nM guide in 95 μl of buffer containing 20 mM Bis–Tris propane, pH 8.0, 50 mM NaCl, 2 mM $MgCl_2$, 0.1% (v/v) Triton X-100 and incubated for 20 min at 37°C. The Ago/guide mixture was combined with 50 nM 5′-FAM labeled substrate (either T-2 or T-3) in a 100 μl cleavage reaction and incubated at 37°C. 10 μl samples were withdrawn from the reaction at the indicated time points and target cleavage was terminated by adding EDTA to a final concentration of 50 mM. Cleavage products at a 4 nM final concentration were separated by capillary electrophoresis (CE) on an Applied Biosystems 3730xl DNA Analyzer (Applied Biosystems, Waltham, MA, USA). The quantitative analysis of fluorescent peaks was performed using PeakScanner Software v1.0 (Thermo Fisher Scientific, Inc., Waltham, MA, USA) and fragment analysis software for in-

house use at New England Biolabs as previously described (34,52).

Argonaute cleavage assays on double-stranded DNA

Synthetic 5′-FAM labeled dsDNA substrates (30, 60 and 100 bp) were generated by combining 1 nmol of the 5′-FAM labeled ss oligonucleotide with 1.25 nmol of the unlabeled complementary oligonucleotide in a 100 μl of 10 mM Tris–HCl buffer, pH 7.5 and incubating for 5 min at 95°C followed by a slow cooling to room temperature. A segment of phage φX174 DNA (3536–3858 nt) was amplified by PCR to generate a 5′-FAM/ROX labeled 322 bp DNA substrate. The PCR product was purified using Monarch PCR and DNA Cleanup kit (New England Biolabs, Inc., Ipswich, MA, USA). DNA concentration was quantified using a NanoDrop spectrophotometer (Thermo Fisher Scientific, Inc., Waltham, MA, USA).

For cleavage of 30, 60 and 100 bp 5′FAM-labeled dsDNA substrates, the CbAgo/guide complex was formed by incubating 0.5 μM CbAgo and 0.5 μM guide B12 for 15 min at 37°C in a 1X CutSmart buffer (50 mM potassium acetate, pH 7.9, 20 mM Tris-acetate, 10 mM magnesium acetate, 100 μg/ml BSA). Cleavage reaction with a final volume of 20 μl was set up in CutSmart buffer containing 50 nM dsDNA substrate, CbAgo:guide complex at a 0.25:0.25 μM final concentration and either 5 μM *E. coli* RecQ or 0.25 μM RecB^{exo-}C. DNA strand unwinding was initiated by adding 5 mM ATP and the reaction was incubated at 37°C for 1 h. The cleavage products at a 4 nM final concentration were analyzed by CE. For one-strand cleavage of 322 bp 5′-FAM/ROX labeled DNA substrate, the CbAgo/guide complex was formed by incubating 0.5 μM CbAgo and 1 μM guide for 15 min at 37°C in a 10 μl of CutSmart buffer. The CbAgo/guide complex at a 0.25/0.5 μM final concentration was combined with 50 nM DNA and 0.5 μM RecB^{exo-}C in a 20 μl of CutSmart buffer and cleavage reaction was initiated at 37°C by adding 5 mM ATP.

For double-strand cleavage experiments, two separate 5 μl reactions, each containing CbAgo (0.5 μM) and a guide (1 μM), were carried out to form CbAgo/guide complexes that target opposing DNA strands. CbAgo/guide complexes, each at the 0.125/0.25 μM final concentration, were combined with 50 nM 322 bp 5′FAM/ROX labeled DNA substrate and 0.25 μM RecB^{exo-}C in a 20 μl of CutSmart buffer and the reaction was initiated at 37°C by adding 5 mM ATP. The cleavage products were analyzed by CE as described above. For time-course experiments, the cleavage reaction volume was increased to 50 μl and 5 μl samples were withdrawn from the reaction at the indicated time points.

Cleavage of φX174, pAd2_BsaI and pAd2_AvrII was carried out using DNA linearized with the appropriate restriction enzyme. Reactions contained 0.2 μg of linear DNA, 5 mM ATP and two CbAgo/guide complexes, each at the 0.125/0.25 μM final concentration, in 20 μl of CutSmart buffer. The CbAgo cleavage was carried out at 37°C for 1 h either in the absence or in the presence of 0.25 μM RecB^{exo-}C. To stop the reaction, samples were supplemented with 50 mM EDTA, 2% SDS and 0.8 units of Proteinase K and were incubated at 25°C for 30 min. Single-stranded CbAgo cleavage products were reannealed by incubating for 5 min at 90°C followed by a slow cooling to 12°C at a rate of 0.1°C/s. Cleavage products were column purified and separated by gel electrophoresis on 1.2% agarose gel. The plasmids pAd2_BsaI and pAd2_AvrII were created by Dr. Richard Morgan (New England Biolabs, Inc., Ipswich, MA, USA) by cloning either a 22 404 bp BsaBI fragment or 19 428 bp AvrII fragment of Adenovirus2 genomic DNA into pUC19 vector.

Ligation of CbAgo-cleaved DNA fragments

A 332 bp 5′-FAM/ROX labeled DNA1 was generated by PCR using a segment of φX174 DNA (nucleotides 3681–4012) as a template. DNA1 was cleaved with CbAgo loaded with guides T2 + B1 to generate a 15 bp 5′-ROX labeled and a 309 bp 5′-FAM labeled cleavage products. A 300 bp 5′-FAM/ROX labeled DNA2 was generated by PCR using a segment of pUC19 DNA (nucleotides 806–1105) as a template. DNA2 was cleaved with CbAgo loaded with guides T5 + B5 to generate a 14 bp 5′-FAM labeled and a 278 bp 5′-ROX labeled cleavage products. All CbAgo cleavage products carried 8-nt long 3′-ss overhangs. The enzymes were inactivated by treatment with Proteinase K for 30 min at 37°C. The 15 and 14 bp fragments were discarded by column purification using Monarch PCR and DNA Cleanup Kit. A 29 bp ds 'Bridge' oligonucleotide was created by combining two complementary 5′-phosphorylated ssDNA oligonucleotides (1 nmol each) in 100 μl of 10 mM Tris–HCl buffer, pH 7.5 and heating for 5 min at 95°C followed by slow cooling down to room temperature. On both ends, the Bridge oligo carried 8-nt long 3′-ss overhangs complementary to the 3′-ss overhangs on the 309 and 278 bp CbAgo cleavage products. DNA fragment ligation was carried out with T4 DNA ligase (400 units) in 10 μl of T4 DNA ligase buffer. First, 0.3 pmol of 309 bp DNA1 fragment and 0.3 pmol of 29 bp Bridge oligonucleotide were ligated for 15 min at 25°C. The reaction was then supplemented with 0.3 pmol of 278 bp DNA2 fragment and ligation continued for another 15 min at 25°C. Ligation products were analyzed by CE.

RESULTS

The search for highly active mesophilic DNA-guided DNA-cleaving Argonautes

The protein sequences of 45 bacterial Agos were aligned, and a phylogenetic tree was built showing inferred evolutionary relationships among pAgo candidates (Supplementary Figure S1A). The search for catalytically active pAgo candidates was carried out in two successive phases. In the initial phase, we randomly selected ten pAgo candidates from more distantly related groups (the candidates are highlighted in yellow in Supplementary Figure S1A). A quick inspection of cleavage activity was performed with candidate pAgo proteins expressed with a PURExpress In Vitro Protein Synthesis kit. Under current conditions, three pAgos (EbAgo, IbAgo and CpAgo) displayed cleavage activity at either 37°C or 65°C temperature, whereas three additional pAgos (PxAgo, KmAgo and PlAgo) were mainly active at 65°C (Supplementary Figure S1B). Ten additional candidates nesting adjacent to the catalytically active pAgos were screened in the second phase (the candidates are highlighted

in orange in Supplementary Figure S1A). Four more candidates (CaAgo, CdAgo, DlAgo and CsAgo) displayed high levels of activity at both 37°C and 65°C, whereas two pAgos (CbAgo and BsAgo) had little or no activity at 37°C but were active at 65°C (Supplementary Figure S1B). Altogether, four pAgo candidates highly active at 37°C were found in hosts that belong to the *Clostridium* genus. The host for a highly active IbAgo was originally assigned as *Clostridium bartlettii*, but later the species was re-assigned as *Intestinibacter bartlettii* (55). Another candidate, CbAgo from *Clostridium butyricum* displayed a residual activity at 37°C but it was attributed to a low level of soluble protein in the PURExpress sample. Upon further inspection, the CbAgo protein was found in a soluble fraction when expressed *in vivo* in T7 Express LysY/I^{q}*E. coli* (Supplementary Methods) and has shown high level of activity at 37°C. Comparative amino acid sequence analysis revealed that the identified Clostridia Argonautes represent a quite diverse group of proteins sharing 61% or less sequence identity, except for CaAgo and CdAgo which have 85% sequence similarity (Supplementary Figure S1C).

To identify the Arogaute with the highest activity at 37°C, we purified and characterized all six pAgo candidates derived from the Clostridia class bacterial hosts. We used a previously described high-throughput CE-based assay (34,52) to rapidly characterize the purified pAgos for guide preference (DNA versus RNA) and target preference (DNA versus RNA). The results are summarized in Supplementary Table S2. Under conditions used in our study, the candidate pAgos preferred DNA guides and DNA targets over RNA guides and RNA targets. CpAgo was the only Argonaute capable of DNA-guided cleavage of RNA and RNA-guided cleavage of DNA, albeit at a reduced rate compared to the DNA-guided DNA cleavage. The candidate pAgos were capable of cleaving DNA at temperatures spanning from 30°C to 80°C (Supplementary Figure S2). In most cases, Ago proteins displayed the highest activity at 50–64°C temperature, except for CpAgo, which was highly active up to 72°C, and for IbAgo, which was the most active at 50°C. The efficiency of DNA target cleavage at 37°C was evaluated at different time points ranging from 5 to 120 min. The results presented in Figure 1 demonstrate that under current conditions the candidate pAgos can be ranked in the following order: CbAgo > CpAgo > CaAgo > CdAgo > IbAgo > CsAgo. Because of the robust activity, CbAgo was considered for analysis of double-stranded DNA cleavage at 37°C in the presence of DNA helicase.

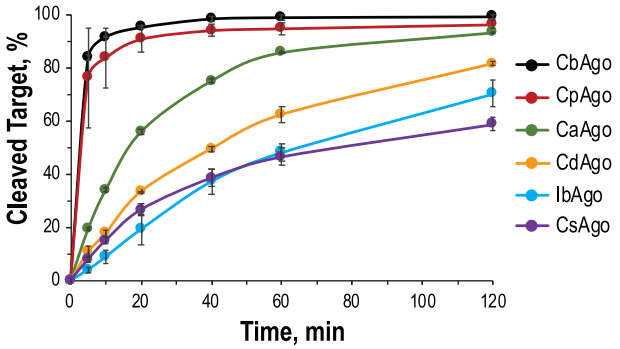

Figure 1. Comparison of *Clostridia* Argonautes for cleavage efficiency of ssDNA target. Cleavage reactions were performed at a final 125:125:50 nM concentration ratio of Ago:Guide:Target as described in Materials and Methods. Error bars indicate the standard deviation of three independent experiments. Bacterial hosts of pAgo proteins used in this study: *C.butyricum* (CbAgo), *C.perfringens* (CpAgo), *C.saudiense* (CaAgo), *C.disporicum* (CdAgo), *I.bartlettii* (IbAgo), *C.sartagoforme* (CsAgo).

The search for DNA helicases that facilitate CbAgo cleavage of linear dsDNA

A review of literature conducted to identify potential helicase candidates revealed that *E. coli* RecQ (EcRecQ) can initiate duplex DNA unwinding from blunt ends if applied at high enzyme-to-DNA molar ratio (56–58). In the presence of 5 μM EcRecQ, CbAgo was proficient in cleaving 30 bp blunt-ended DNA (Figure 2A, lane 3). However, the CbAgo cleavage efficiency steadily declined when the length of DNA substrate was increased to 60–100 bp (Figure 2A, lanes 4–5). No CbAgo cleavage activity was detected on longer than 100 bp dsDNA substrates indicating that EcRecQ is not suitable for programmable cleavage of long dsDNAs.

The RecBCD enzyme has been considered as another potential DNA helicase given that it prefers unwinding blunt or nearly blunt-ended DNA (42). The studies of individual constituent subunits and their combinations have indicated that the RecB subunit alone is a weak DNA helicase, but the DNA unwinding activity is significantly increased upon interaction with the RecC subunit (42,43,49). The RecBC enzyme, lacking the RecD subunit, is about 4-fold slower and less processive than the RecBCD enzyme, but still has been shown to completely unwind 6.25–21.4 kb linear DNAs in a matter of minutes (50). We have constructed a nuclease deficient variant of the RecB helicase referred to as RecB^{exo-}, by replacing three catalytic residues, E1020, D1080 and K1082 with alanine residue. Individually purified RecB^{exo-} and RecC subunits were mixed at a 1:1 stoichiometry to reconstitute the RecB^{exo-}C helicase. DNA unwinding activity of either RecB^{exo-} or RecB^{exo-}C was tested using the CE-based assay as described in Supplementary Methods. The obtained results have confirmed that the RecB^{exo-} subunit alone is a weak DNA helicase compared to the RecB^{exo-}C complex which displayed a quite robust DNA unwinding activity (Supplementary Figure S3). The nuclease deficient RecB^{exo-}C helicase was then explored as a CbAgo partner for cleavage of dsDNA at 37°C. In contrast to EcRecQ, DNA strand unwinding by the RecB^{exo-}C helicase has led to a complete CbAgo cleavage of 30–100 bp DNA substrates, thus implying that CbAgo and RecB^{exo-}C combination has the potential for programmable dsDNA cleavage (Figure 2B).

RecB^{exo-}C DNA helicase assists CbAgo in cleaving targets on 322 bp linear dsDNA

To further investigate CbAgo cleavage activity on dsDNA, we designed the 21-nt long guides T2 and B2 to target opposing DNA strands in the middle of a 322 bp 5′-FAM/ROX labeled DNA substrate (Figure 3A). The targeted DNA region contained a BbvCI restriction site al-

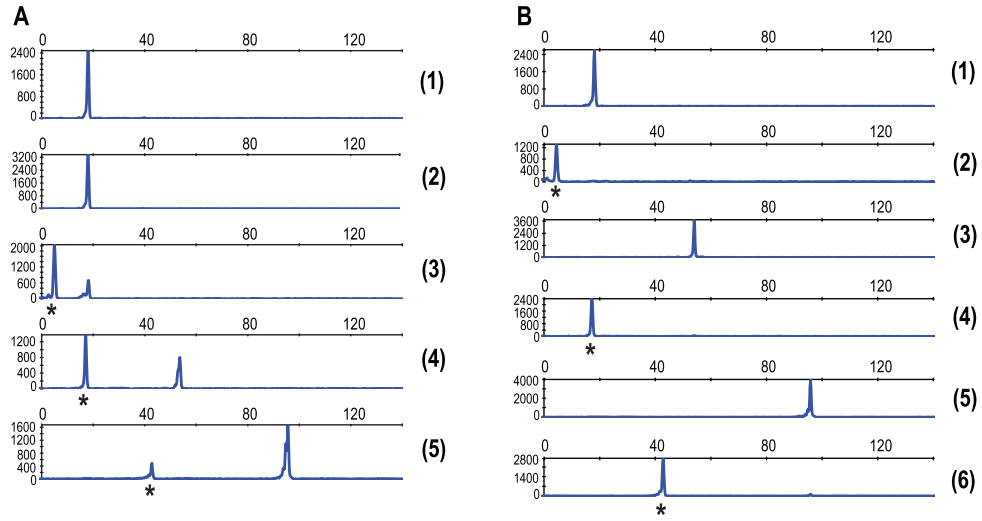

Figure 2. Effect of the helicase-catalyzed DNA strand unwinding on the double-stranded DNA cleavage by CbAgo. CbAgo was loaded with a guide B12 at a 1:1 CbAgo:guide molar ratio to form a CbAgo/B12 complex. Either 30 bp, 60 bp or 100 bp 5′-FAM labeled blunt-ended dsDNA substrates were cleaved at 37°C for 1 h with the CbAgo/B12 complex either in the absence or in the presence of DNA helicase. 5′-FAM labeled cleavage products were analyzed by capillary electrophoresis as described in Materials and Methods. CbAgo cleavage products are marked with an asterisk (*). (**A**) CbAgo cleavage activity in the presence of *E. coli* RecQ DNA helicase. Lane 1, 30 bp DNA. Lane 2, 30 bp DNA incubated with the CbAgo/B12 complex. Lanes 3–5, 30, 60 and 100 bp DNA, respectively, was cleaved with the CbAgo/B12 complex in the presence of *E. coli* RecQ DNA helicase. (**B**) CbAgo cleavage activity in the presence of the RecB^{exo-}C DNA helicase. Lanes 1, 3 and 5, 30, 60 and 100 bp DNA was incubated with the CbAgo/B12 complex, respectively. Lanes 2, 4 and 6, 30, 60 and 100 bp DNA was cleaved with the CbAgo/B12 complex in the presence of the RecB^{exo-}C DNA helicase.

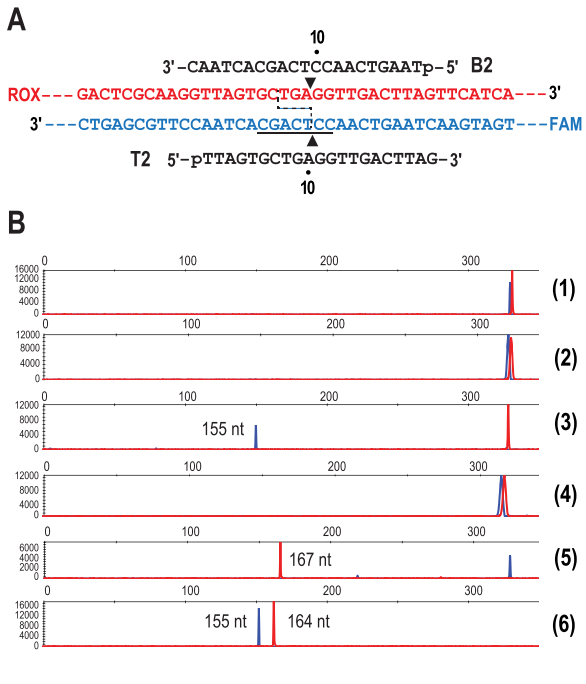

Figure 3. Guide-specific cleavage of double-stranded DNA by CbAgo in the presence of RecB^{exo-}C helicase. (**A**) Schematic overview of guide positioning on a 5′-FAM/ROX labeled 322 bp dsDNA substrate. Black triangles indicate cleavage positions of the CbAgo/B2 and CbAgo/T2 complexes. The BbvCI recognition site is underlined, and dashed lines show BbvCI cleavage positions. (**B**) Capillary electrophoresis results. Lane 1, dsDNA substrate. Lane 2, dsDNA cleaved with CbAgo/T2. Lane 3, dsDNA cleaved with CbAgo/T2 in the presence of RecB^{exo-}C. Lane 4, dsDNA cleaved with CbAgo/B2. Lane 5, dsDNA cleaved with CbAgo/B2 in the presence of RecB^{exo-}C. Lane 6, dsDNA cleaved with 10 units of BbvCI restriction endonuclease.

lowing the use of BbvCI restriction fragments as internal markers to verify the size of CbAgo cleavage products. In the absence of RecB^{exo-}C helicase no cleavage was observed after DNA was treated with either CbAgo/T2 or CbAgo/B2 (Figure 3B, lanes 2 and 4, respectively). The result was expected as CbAgo by itself cannot initiate guide-specific cleavage of duplex DNA. However, when the CbAgo reaction was supplemented with RecB^{exo-}C, either the CbAgo/T2 or CbAgo/B2 complex cleaved 322 bp DNA in a guide-specific mode as confirmed by the appearance of 155 nt 5′-FAM labeled and 167 nt 5′-ROX labeled cleavage products (Figure 3B, lanes 3 and 5). The size of the CbAgo generated fragments was verified by the BbvCI cleavage, which produced a 5′-FAM labeled 155 nt and a 5′-ROX labeled 164 nt fragments (Figure 3B, lane 6). In addition, the CbAgo-cleaved DNA fragments were directly sequenced to confirm that CbAgo indeed cleaved a phosphodiester bond positioned between the nucleotides 10 and 11 if counting from the guide 5′-end (Supplementary Figure S4).

An array of 21-nt long DNA guides was used to evaluate CbAgo efficiency for cleavage of single strands within 322 bp dsDNA in the presence of RecB^{exo-}C helicase. Four guides designed to cleave a 5′-ROX labeled strand (Supplementary Figure S5A) resulted in very efficient CbAgo/guide complexes as 50–80% of the respective targets were cleaved in the first 4 min, and 95–100% cleavage was achieved after 16 min at 37°C (Supplementary Figure S5B). Sixteen guides were designed to hybridize with the 5′FAM-labeled strand at sequences that were shifted by one nucleotide with respect to each other (Supplementary Figure S6A). This strand was cleaved significantly slower, and only ten CbAgo/guide complexes could cleave the respective targets more than 50% in 16 min (Supplementary Figure S6B). Except for the guides A1 and T1-C1, CbAgo

loaded with different guides cleaved the respective targets up to 80–100% in 64 min. Despite the observed differences, the results provided strong evidence that CbAgo can rapidly find and cleave transiently formed ssDNA targets embedded on long dsDNA during ongoing strand unwinding by RecB^{exo-}C helicase.

Effect of CbAgo:guide molar ratio on double-strand DNA cleavage

Two guide pairs were initially selected to test the double-strand cleavage of a 322 bp dsDNA in the presence of RecB^{exo-}C helicase. Double-strand cleavage by CbAgo loaded with guides T2 and B1 was expected to generate DNA fragments tailed with 5nt-long 3′-ss overhangs. In contrast, CbAgo loaded with guides T1-C2 and B4 was expected to generate DNA fragments tailed with 5nt-long 5′-ss overhangs (left panels in Figure 4). CbAgo was pre-loaded with individual guides, then two CbAgo/guide complexes were combined in the reaction with dsDNA and RecB^{exo-}C helicase, and cleavage of each DNA strand was monitored over time. Concurrent cleavage of DNA strands by CbAgo/T2 and CbAgo/B1 rapidly advanced to completion (Figure 4A). Unexpectedly, a ∼10-fold decline in cleavage of either DNA strand was observed when CbAgo was loaded with T1-C2 and B4 guides, which were arranged to generate a 5′-staggered double-strand break (Figure 4B). The cleavage of either DNA strand remained profoundly incomplete after 64 min in contrast to the respective single-guided cleavage reactions (Supplementary Figures S5 and S6).

To further explore the observed bias, CbAgo efficiency was compared in a series of experiments using two sets of guide pairs created by combining guides B1 and B4 targeting a 5′-ROX labeled strand with 16 guides targeting a 5′-FAM labeled DNA strand. The use of 16 guides combined with either guide B1 or guide B4 allowed to generate CbAgo cleavage products tailed with either 3′-ss overhangs or 5′-ss overhangs varying from 0 to 15 nt in length, respectively (Figure 5A). CbAgo efficiently cleaved dsDNA when loaded with guides programmed to create 3′-staggered double-stranded breaks resulting in 80–100% DNA strand cleavage after 16 min at 37°C (Figure 5B). In numerous cases, DNA strand cleavage was significantly reduced when CbAgo was loaded with guides arranged to generate cleavage products with 5′-ss overhangs (Figure 5C). The largest decline was observed with guide pairs positioned to generate 5′-ss overhangs varying from 5 nt to 8 nt in length. However, CbAgo activity partially recovered when a 5′-ss overhang was increased from 9 nt to 15 nt (Figure 5C).

Under current reaction conditions, CbAgo was loaded with each guide at a 1:2 Ago:guide molar concentration ratio with the intention of avoiding a non-specific DNA 'chopping' by a guide-free CbAgo (23–25). Such arrangement indicates double-strand cleavage is carried out in the presence of free guides that highly complement each other. We then postulated that free guides potentially might interfere with dsDNA cleavage when guides are arranged to generate 5′-staggered double-stranded breaks. To verify this prediction, a detailed analysis of varying CbAgo:guide molar concentration ratios was performed using a T1-A1 + B4 guide pair (Figure 6). Double-strand cleavage by CbAgo/T1-A1 + B4 was virtually eliminated when CbAgo was loaded with guides at the Ago:guide molar ratios ranging from 1:2 (125:250 nM) to 1:1.8 (125:225 nM). Interestingly, CbAgo activity increased when the Ago:guide molar ratio was gradually reduced from 1:1.6 (125:200 nM) to 1:1.2 (125:150 nM), and at a 1:1 molar ratio (125:125 nM) more than 90% cleavage of both strands was achieved after 16 min at 37°C (Figure 6). Next, CbAgo was loaded at the 1:1 molar ratio with 16 guide pairs arranged to produce dsDNA fragments with 5′-ss overhangs of varying length. Remarkably, an efficient cleavage of both DNA strands was observed with all guide pairs when cleavage reactions were performed using equimolar CbAgo and guide concentrations (Supplementary Figure S7).

The results clearly indicate that CbAgo activity is inhibited by the presence of free guides in the reaction, but only if the guides are arranged to generate products with 5′-ss overhangs. In contrast, no inhibition occurs if a 2-fold molar excess of guides over CbAgo is used to generate double-stranded cleavage products tailed with 3′-ss overhangs (Figure 5B). In summary, we have demonstrated here that in the presence of RecB^{exo-}C helicase, CbAgo can efficiently cleave dsDNA and produce DNA fragments flanked with either 3′- or 5′-ss overhangs of varying length. Still, a correct Ago:guide molar ratio must be used when aiming to create cleavage products tailed with 5′-ss overhangs.

CbAgo acts as a programmable DNA-guided endonuclease on linear double-stranded DNA

The linearized 5.4 kb φX174 phage DNA was used to explore if CbAgo/RecB^{exo-}C can cleave substantially longer dsDNA at 37°C. Previous studies have shown that *E. coli* RecBC helicase has preference for double-stranded DNA substrates with 3′-ss overhangs compared to blunt ends or 5′-ss overhangs (49). To investigate the effect of DNA end structure on the CbAgo/RecB^{exo-}C cleavage, five linear DNA substrates were generated by cleaving φX174 DNA with unique restriction endonucleases: SspI or StuI cleavage generated blunt ends, SapI or XhoI cleavage generated 5′-ss overhangs and AatII cleavage generated 3′-ss overhangs. CbAgo targets were selected in the middle of the respective linear DNAs to produce two similar in size DNA fragments which could run as a single band during agarose gel-electrophoresis (Figure 7A). All DNA guides were designed with a 5′-T terminal nucleotide for a few reasons. First, a comparison of various single-guided cleavage reactions showed that guides carrying either 5′-G or 5′-T terminal nucleotides resulted in more uniform cleavage efficiencies compared to the guides with a 5′-A or a 5′-C terminal nucleotide (Supplementary Figures S5 and S6). Second, all guides pairs were intentionally planned to generate 5nt-long 3′-ss overhangs at the CbAgo cleavage sites to ensure that the antiparallel guides complement each other by the same number of nucleotides. However, the analysis of φX174 nucleotide sequence revealed that only the guides starting with a 5′-T terminal nucleotide were available at all targeted locations.

In the presence of RecB^{exo-}C, CbAgo efficiently cleaved linear φX174 DNA at all five targeted locations (Figure

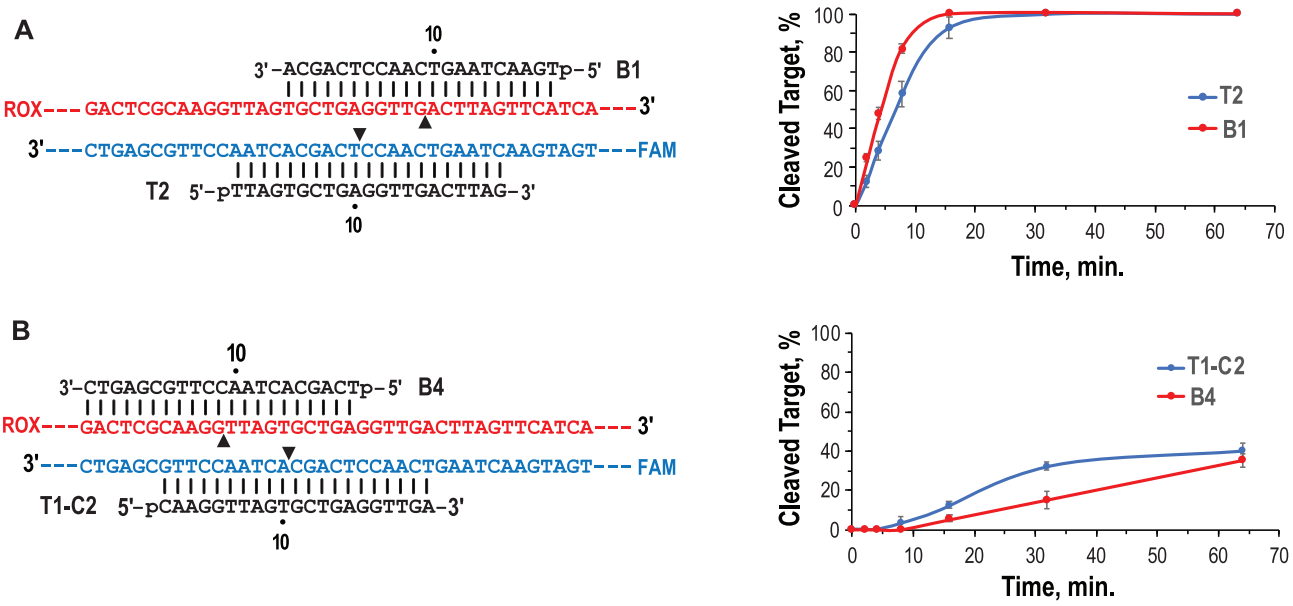

Figure 4. Double-strand cleavage of the 5′-FAM/ROX labeled 322 bp DNA by CbAgo loaded with a guide pair T2 + B1 (**A**) or T1-C2 + B4 (**B**) in the presence of RecB^{exo-}C. Panels on the left show the targeted region of 322 bp dsDNA substrate and guides used for cleavage of DNA strands. Black triangles show target cleavage sites. DNA cleavage was carried out at 37°C in the presence of 250 nM RecB^{exo-}C, and samples were removed from the reaction after 2, 4, 8, 16, 32 and 64 min. Cleavage products were analyzed by CE and quantified as described in Materials and Methods. Error bars indicate standard deviation of three independent experiments. (**A**) Time-course of double-strand cleavage with CbAgo/T2 + B1, which generates DNA fragments flanked with 5-nt long 3′-ss overhangs. (**B**) Time-course of double-strand cleavage with CbAgo/T1-C2 + B4, which generates DNA fragments flanked with 5-nt long 5′-ss overhangs.

7A, lane 2 in panels I–V). The specificity of DNA-guided cleavage was confirmed by cleaving a SspI-linearized φX174 DNA with SapI, which produced restriction fragments similar in size to DNA fragments generated by CbAgo/T2 + B1 (Figure 7A, lane 3). The results demonstrate that the RecB^{exo-}C helicase can efficiently unwind 5.4 kb dsDNA regardless of the linear DNA end configuration, thus promoting CbAgo cleavage of transiently formed single-stranded targets. A closer inspection, however, revealed that DNA cleavage by CbAgo programmed with guide pairs T2 + B1 and XhoT + XhoB (panels I and II) was more efficient than at the other three locations, which were targeted with StuT + StuB, SapT + SapB or AatT1 + AatT2 guide pairs (panels III–V, respectively). To further investigate whether cleavage efficiency was affected by the guide sequence, the same locus of the AatII-linearized φX174 DNA was targeted with CbAgo loaded with four pairs of guides carrying different 5′-terminal nucleotides (Supplementary Figure S8A). Complete DNA cleavage was achieved with the guide pairs AatG1 + AatG2 and AatA1 + AatA2 carrying either a 5′-G or a 5′-A terminal nucleotide, respectively (Supplementary Figure S8B, lanes 2–3), whereas DNA cleavage was slightly less efficient with AatT1 + AatT2 and AatC1 + AatC2 guide pairs which started with either a 5′-T or a 5′-C terminal nucleotide (lanes 4–5). Taken all together, the results did not reveal a strong bias for a 5′-terminal nucleotide as the cleavage efficiency was quite prominent for all tested guide pairs. Nevertheless, the observed variability in the endonucleolytic activity suggest that CbAgo exhibits flexible preferences for guides with the particularly arranged nucleotide combinations.

A mesophilic Ago activity has never been demonstrated on dsDNA longer than 5–6 kb. To determine if CbAgo/RecB^{exo-}C combination can cleave 20–25 kb DNA at 37°C, the plasmids pAd2_BsaBI (22.114 kb) and pAd2_AvrII (25.091 kb) were linearized with AscI and SrfI, respectively, and two guide pairs were designed to target each DNA at a midpoint (Figure 7B and C). In the presence of RecB^{exo-}C, CbAgo loaded with the respective guide pair specifically cleaved targeted sites as indicated by the appearance of 11 and 12.5 kb cleavage products (lane 2 in Figure 7B and C, respectively). Remarkably, the concurrent DNA unwinding by RecB^{exo-}C permits CbAgo to cleave DNA targets located at an 11–12.5 kb distance from the end of dsDNA.

We also investigated whether five other Clostridia Argonautes described in this study can cleave linear dsDNA in the presence of RecB^{exo-}C DNA helicase (Supplementary Figure S9). Only CpAgo displayed a robust activity at all three targeted sites of φX174 DNA, albeit with a lower efficiency compared with CbAgo. The remaining four pAgos (CaAgo, CdAgo, CsAgo and IbAgo) displayed greatly reduced levels of dsDNA cleavage. The observed dsDNA cleavage patterns were consistent with the ssDNA cleavage results which established CbAgo and CpAgo as the two fastest pAgos among the six tested candidates (Figure 1). Taken together, these results imply that pAgos exhibiting fast cleavage rates are best suited for efficient cleavage of dsDNA, apparently because they can cleave transiently formed single-stranded targets faster than the reannealing of DNA strands occurs at physiological temperature.

Finally, the ability of CbAgo/RecB^{exo-}C to cleave a supercoiled form of DNA at 37°C was investigated at three

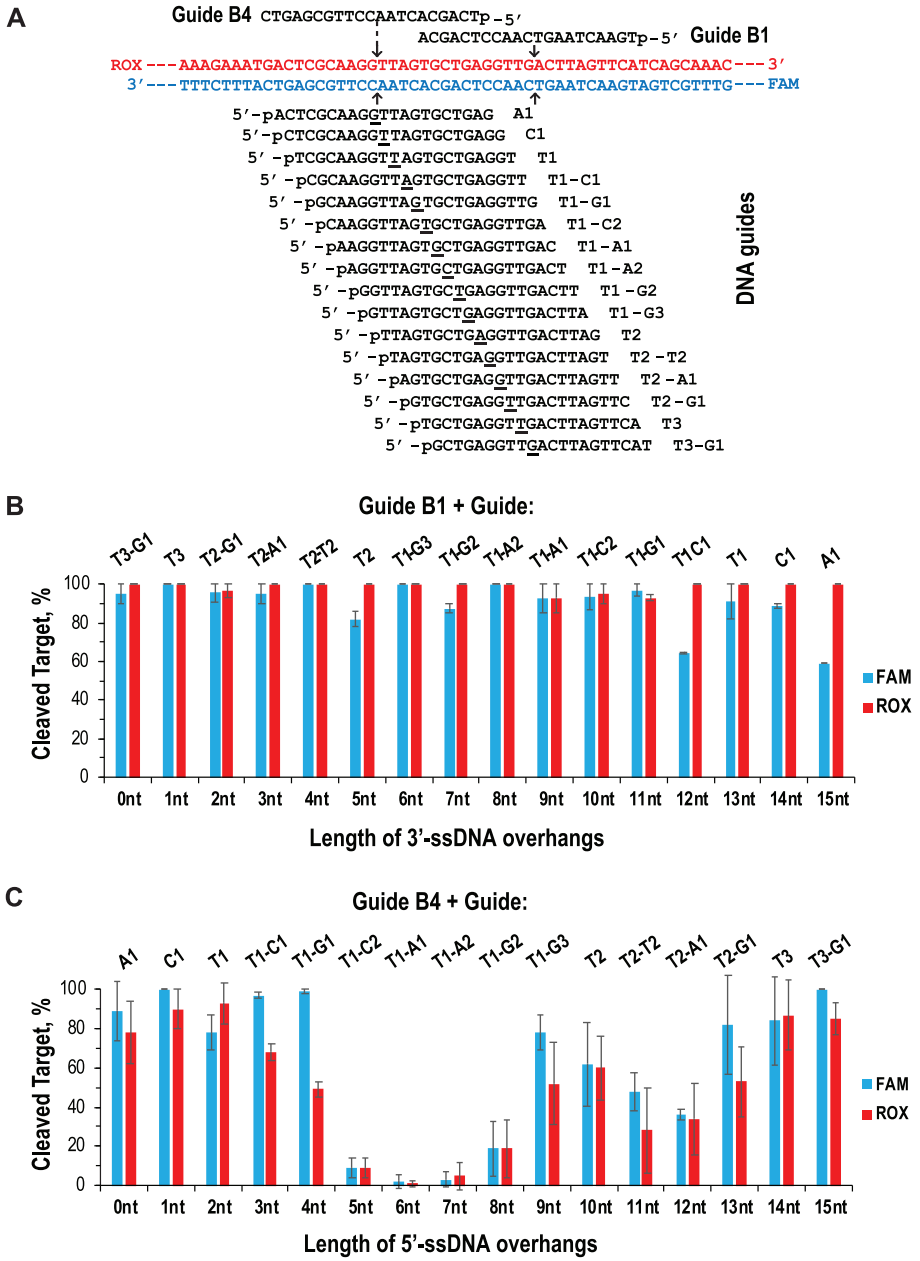

Figure 5. Double-strand cleavage of the 5′-FAM/ROX labeled 322 bp DNA by CbAgo loaded with two sets of 16 guide pairs which generate cleavage products tailed with either 3′- or 5′-ss overhangs. (**A**) Schematic overview of guide positioning on DNA target. Within each guide sequence, the 10th nucleotide starting from a 5′-phosphate is underlined to mark position that aligns with the CbAgo cut site. On the 5′-FAM labeled strand, arrows indicate cleavage position of the first (CbAgo/A1) and the last (CbAgo/T3-G1) complexes. CbAgo/guide complexes were combined with dsDNA substrate at the CbAgo:guide:target concentration ratio of 125:250:50 nM. The concurrent double-strand cleavage was carried out for 16 min at 37°C in the presence of 250 nM RecB^{exo-}C. The percentage of cleaved DNA was quantified for each DNA strand. (**B**) Efficiency of double-strand cleavage by CbAgo loaded with the indicated guide pairs which generate cleavage products tailed with 3′-ss overhangs varying from 0 to 15 nt in length. Error bars indicate the standard deviation of two independent experiments. (**C**) Efficiency of double-strand cleavage by CbAgo loaded with the indicated guide pairs which generate cleavage products tailed with 5′-ss overhangs varying from 0 to 15 nt in length. Error bars indicate the standard deviation of three independent experiments.

φX174 DNA locations. In contrast to linear dsDNA, no nicking/cleavage of supercoiled φX174 DNA by either CbAgo or CbAgo/RecB^{exo-}C was observed after a 16-h incubation at 37°C, thus confirming that RecB^{exo-}C DNA helicase cannot unwind a circular DNA (Supplementary Figure S10).

PCR-free method for seamless assembly of DNA fragments by using CbAgo and RecB^{exo-}C

Capitalizing on the success of programmable linear dsDNA cleavage by CbAgo/RecB^{exo-}C, we considered a method for seamless assembly of CbAgo-cleaved DNA fragments. Since Argonaute cleaves DNA strands in two independent

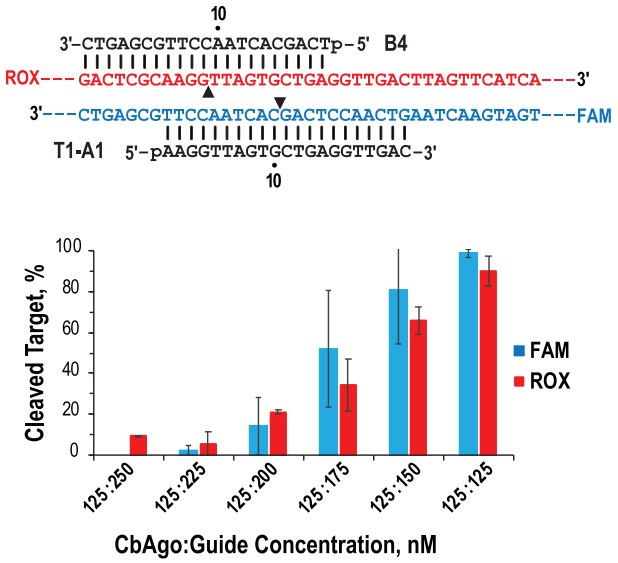

Figure 6. Efficiency of double-strand cleavage of the 5′-FAM/ROX labeled 322 bp DNA at different CbAgo:guide molar concentration ratios. CbAgo/T1-A1 and CbAgo/B4 complexes were combined with dsDNA target at the CbAgo:guide:target concentration ratios of 125:250:50, 125:225:50, 125:200:50, 125:175:50, 125:150:50 and 125:125:50 nM. Double-strand cleavage was carried out for 16 min at 37°C in the presence of 250 nM RecB^{exo-}C helicase, and the percentage of cleaved DNA was quantified for each DNA strand. Error bars indicate standard deviation of three independent experiments.

events, a double-strand cleavage offers strategic advantages. The most efficient cleavage sites can be selected close to the end of targeted DNA and ssDNA overhangs of preferred length and composition can be created to facilitated DNA assembly. A synthetic dsDNA oligonucleotide equivalent to the two cleaved-off terminal fragments then can be used to directionally link two DNA fragments via complementary single-stranded overhangs (Figure 8A).

As a proof-of-principal, we assembled 332 and 300 bp 5′-FAM/ROX labeled PCR fragments (referred to as DNA1 and DNA2, respectively). On DNA1, the CbAgo target site was selected close to the 5′-ROX labeled end, whereas on DNA2 the CbAgo target site was selected close to the 5′-FAM-labeled end (Figure 8A). The guide pairs T1 + B2 and T5 + B5 complemented DNA1 and DNA2, respectively, and both guide pairs were arranged to create 8nt-long 3′-ss overhangs on the CbAgo cleavage products. In this arrangement, the CbAgo cleavage of either DNA produced throwaway terminal fragments, a 5′-ROX labeled 15 bp fragment and a 5′-FAM labeled 14 bp fragment, which were eliminated by column purification (Figure 8B). DNA1 and a synthetic 29 bp 'Bridge' oligonucleotide were then ligated for 15 min at 25°C to generate a 346 bp intermediate ligation product. The ligation reaction was then supplemented with DNA2, and ligation continued for another 15 min. Results presented in Figure 8B reveal the formation of 346 bp 5′-FAM labeled ligation product during the first ligation step. The formation of 632 bp 5′-FAM/ROX labeled ligation product during the second ligation step indicates that both CbAgo cleavage products and Bridge oligonucleotide were directionally assembled into a recombinant DNA. Both strands of the final ligation product were sequenced to inspect nucleotide sequences at the ligation junctions. Sequencing data confirmed that the CbAgo-generated single-stranded overhangs were precisely ligated with the complementary ss overhangs of the Bridge oligonucleotide (Supplementary Figure S11). The results provided a compelling evidence that CbAgo cleavage produces DNA fragments with sequence-specific ssDNA overhangs that are ready for ligation without any further enzymatic treatment. These findings confirm that seamless assembly of linear DNA molecules can be accomplished using CbAgo/RecB^{exo-}C programmable DNA endonuclease.

DISCUSSION

The *in vitro* mechanism of dsDNA cleavage was first established for thermophilic pAgos that act in a range of temperatures that trigger thermal DNA destabilization (21,26,33). The model demonstrates that pAgo nuclease can cleave dsDNA in two independent events if two pAgo/guide complexes are used to target antiparallel DNA strands (33). Mesophilic pAgos *in vitro* act poorly on double-stranded substrates because they are unable to invade DNA duplex. Many studies have shown that only plasmids with destabilized double-stranded regions can be targeted by mesophilic pAgos at 25–40°C temperatures suggesting that *in vivo* pAgos potentially rely on natural processes that involve strand separation (25,27,28,35–37). In this study, we explored the possibility of using DNA helicases to initiate single-stranded target cleavage by a mesophilic pAgo at physiological temperature. We demonstrated that DNA strand unwinding by nuclease deficient helicase RecB^{exo-}C allows Argonaute CbAgo from *Clostridium butyricum* to cleave linear dsDNAs ranging from 30 to 25 kb in length.

The approach of combining CbAgo with the RecB^{exo-}C helicase provides an unprecedented opportunity to *in vitro* investigate DNA-guided cleavage of dsDNA at 37°C. We used a high-throughput capillary electrophoresis technique to compare many CbAgo/guide complexes for cleavage of either one or both DNA strands. In our study, 16 DNA guides were designed to hybridize with DNA targets at positions shifted by one nucleotide with respect to each other. Such guide sequence design allowed to change a 5′-terminal nucleotide and to shift the CbAgo cleavage position along the substrate DNA. Some variability in cleavage efficiency was detected with different guides, but overall, CbAgo was able to cleave DNA targets regardless of the nature of a 5′-nucleotide and regardless of the combination of nucleotides at the 10th and 11th positions involved in the coordination of the scissile phosphodiester bond cleavage (Figure 5B, Supplementary Figures S7 and S8). Our results were consistent with the CbAgo cleavage results previously observed on single-stranded targets showing no strong preference for a 5′-terminal nucleotide (25,35,51). In some cases, however, DNA cleavage efficiency was noticeably affected by a minimal shift of guide sequence along the targeted DNA (Supplementary Figure S6). Recently a large-scale systematic study of guide preference was performed for TtAgo, revealing activity correlation with the 1st and 12th base of the guide and, to a lesser degree, with the bases surrounding the cut site (59). Potentially, a similar large-scale study performed with the CbAgo/RecB^{exo-}C combination could

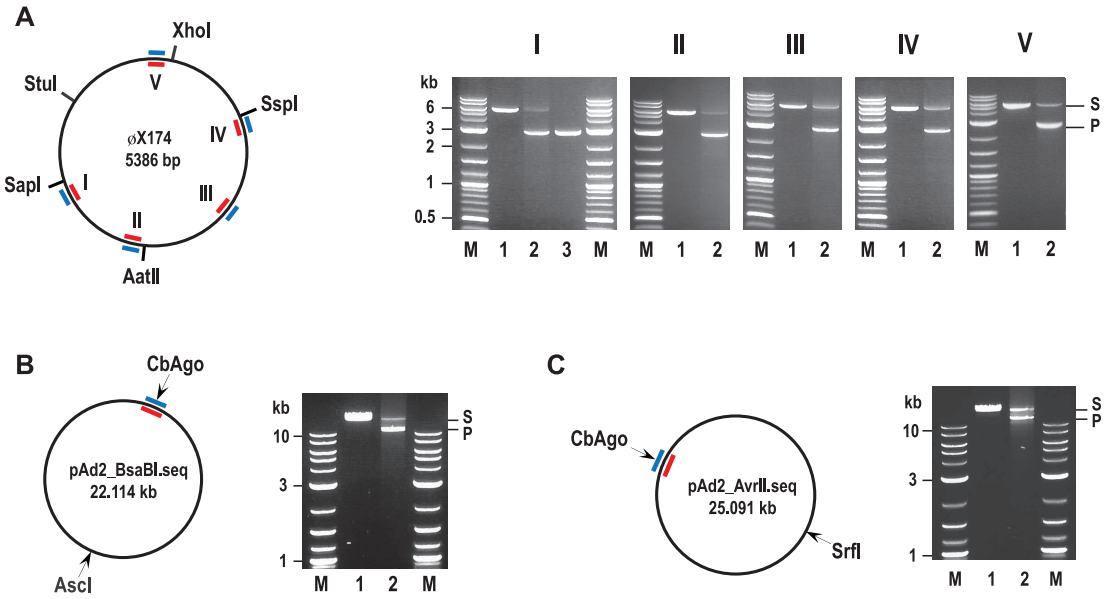

Figure 7. CbAgo acts as a programmable DNA endonuclease on linear dsDNA. DNA cleavage by CbAgo was carried out either in the absence (Lane 1) or in the presence of RecB^{exo-}C (Lane 2). The circular map of dsDNA substrate with restriction sites and guide positions is shown on the left of the respective gel. (**A**) Five locations of linear φX174 DNA were targeted with CbAgo loaded with five different guide pairs. Panel I, SspI-linearized DNA cleaved with CbAgo/T2 and CbAgo/B1. Lane 3, SspI + SapI digested DNA. Panel II, XhoI-linearized DNA cleaved with CbAgo/XhoT and CbAgo/XhoB. Panel III, StuI-linearized DNA cleaved with CbAgo/StuT and CbAgo/StuB. Panel IV, SapI-linearized DNA cleaved with CbAgo/SapT and CbAgo/SapB. Panel V, AatII-linearized DNA cleaved with CbAgo/AatT1 and CbAgo/AatT2. (**B**) AscI-linearized pAd2_BsaBI DNA (22 114 bp) cleaved with CbAgo/AdB-450T and CbAgo/AdB-450B. (**C**) SrfI-linearized pAd2_AvrII DNA (25,091 bp) cleaved with CbAgo/AdA-20860T and CbAgo/AdA-20860B. S, linear DNA; P, CbAgo cleavage products; M, 1 kb plus DNA ladder.

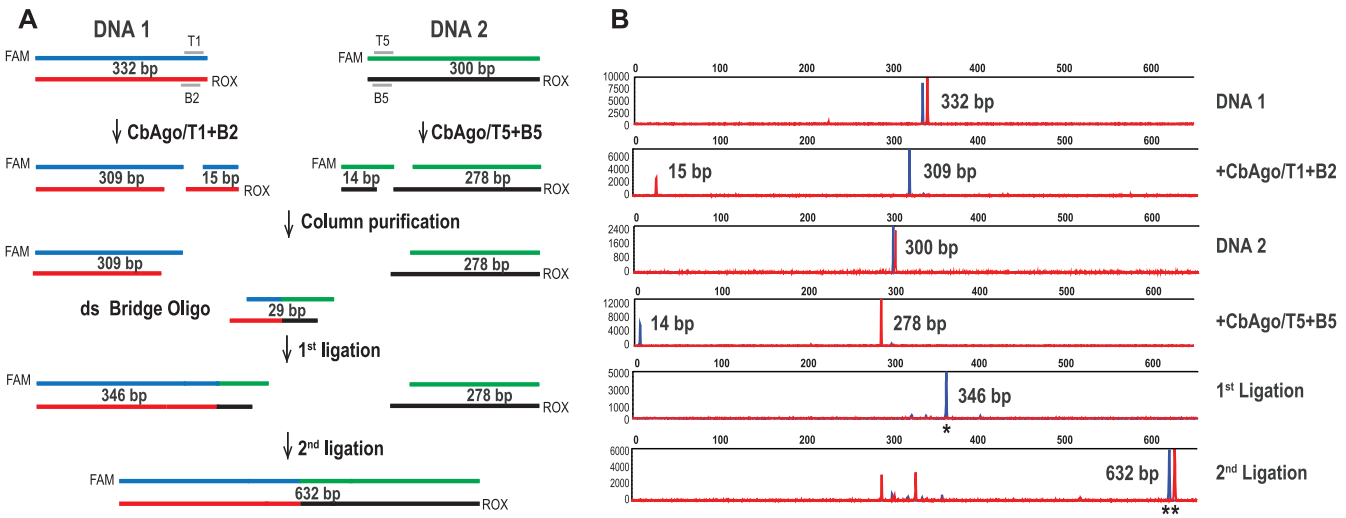

Figure 8. Seamless and directional assembly of dsDNA fragments using CbAgo and RecB^{exo-}C. (**A**) Schematic overview of a seamless DNA assembly method. CbAgo/guide cleavage was carried out in the presence of RecB^{exo-}C DNA helicase as described in Materials and Methods. (**B**) CE analysis of CbAgo cleavage and ligation products. Ligated fragments are marked with an asterisk (*).

lead to a better understanding of some basic principles that must be followed to optimize the guide sequences for programmable dsDNA cleavage.

The concurrent cleavage of DNA strands permits generation of custom-designed cleavage products by choosing the length and polarity of single-stranded overhangs (i.e. 5′- or 3′-ss overhang). CbAgo was found to efficiently cleave both DNA strands if guide pairs were prearranged to generate fragments tailed with 3′-ss overhangs. But dsDNA cleavage was significantly reduced if the guide pairs were designed to generate 5′-ss overhangs (Figure 5). A comprehensive study of varying CbAgo:guide molar ratios revealed that presence of free guides might inhibit dsDNA cleavage when the opposing CbAgo/guide complexes are arranged to generate a 5′-staggered double-strand break. Our results indicate that inhibition can be circumvented by loading CbAgo with guides at the Ago:guide molar ratios ranging from 1:1.4 to 1:1 (Figure 6 and Supplementary Figure S7).

The sequence alignment of antiparallel guides targeting complementary DNA strands shows that the guides must have complementary 5′-terminal sequences to generate cleavage products with 5′-ss overhangs (Figure 5A). The 5′-terminus of a guide plays a crucial role in target recognition and cleavage by Ago nuclease. Nucleotides 2–8 of the guide counted from a 5′-end are termed the 'seed' region. In an Ago/guide complex, the bases of the seed region are solvent-exposed, therefore they can readily base pair with a matching sequence on the target strand (12,60,61). The crystal structure of CbAgo in complex with a guide and complementary target reveals a 15 base pair duplex formed by nucleotides 2–16 of a guide and a target (35). This evidence implies that at least a 16-nt long target is anticipated for a CbAgo/guide/target complex to adopt a catalytically favored configuration. Minimal target length requirements were investigated for TtAgo loaded with a 21-nt guide DNA. The study showed that truncation of the target to 16 nt did not alter TtAgo cleavage activity, but 15- and 14-nt targets showed 120- and 400-fold reduced cleavage rates, respectively, and a 12-nt target was not cleaved (17). This information allows us to rationalize the dsDNA cleavage results when guides are provided in excess of CbAgo. If two opposing guides complement each other by 5′-terminal sequences, then the seed region of one CbAgo/guide complex might base pair with the opposing free guide, thus forming a 'CbAgo/guide/free-guide' complex. At the initial reaction phase, CbAgo may then promptly cleave the guides bound as single-stranded targets instead of dsDNA targets that are yet to be unwound. A delayed target cleavage of at least one DNA strand was observed with guide pairs having 5′-complementary sequences longer than 16 nucleotides. Surprisingly, dsDNA cleavage was severely inhibited when CbAgo/guide complexes and free opposing guides were capable of base pairing by 12–15 nucleotides (Figures 4B and 5C). These results suggest that guides bound as 12–15 nt long targets can be either cleaved at significantly reduced rates or cannot be cleaved at all. Considering that product release is the limiting reaction step (25,35), the release of the 12–15 nt-long uncut targets is likely an extremely slow process resulting in an accumulation of catalytically impaired 'CbAgo/guide/free-guide' complexes which no longer useful for dsDNA cleavage.

For efficient double-strand cleavage, CbAgo must be loaded with guides at a 1:1 molar ratio if two CbAgo/guide complexes are arranged to generate a 5′-staggered break (Figure 6). However, the use of equimolar CbAgo:guide concentration may result in accumulation of a guide-free CbAgo, which may damage sequence-specific ends of dsDNA due to the inherent non-specific nuclease activity associated with the guide-free Ago (23–25). This problem can be circumvented by using guides programmed to generate 3′-ss staggered double-stranded breaks as dsDNA cleavage efficiency is unaffected by the CbAgo:guide molar ratio. This is because the opposing guides complement each other on their 3′-ends, resulting in a 5′-terminal seed region of the Ago/guide complex that lacks a matching complementary sequence for initial binding of free guide. We have shown that CbAgo loaded with guides at a 1:2 molar ratio efficiently generates DNA fragments with 8nt-long 3′-ss overhangs which are ready for ligation without any further enzymatic treatment (Figure 8).

Two enzymatic qualities are essential for efficient cleavage of double-stranded DNA at physiological temperature: a rapid and processive DNA strand separation and a rapid cleavage of transiently formed ssDNA targets. The RecBCD enzyme is the most rapid and processive DNA helicase (47). The RecBC enzyme lacking the RecD subunit was also shown to act as a fast and processive DNA helicase capable of unwinding up to 20 kb dsDNA, although its unwinding speed and processivity is lower than that of the RecBCD helicase (48–50). We have demonstrated here that with the help of RecB^{exo-}C DNA helicase, a mesophilic CbAgo can efficiently cleave linear dsDNAs up to 25 kb in length. However, future studies will be needed to investigate if the RecB^{exo-}CD enzyme can further increase CbAgo cleavage efficiency, especially on longer than 25 kb dsDNA. Our results indicate that Argonautes which rapidly cleave ssDNA targets are also the most efficient in dsDNA cleavage at physiological temperature (Figure 1, Supplementary Figure S9). This comes as no surprise, as Argonaute has very limited time to both find and cleave the short-lived single-stranded targets before complementary DNA strands reanneal back together. Under current conditions, all investigated Clostridia pAgos, including CbAgo, displayed a significantly higher activity at temperatures ranging from 50°C to 64°C than at 37°C (Supplementary Figure S2). This implies that there are still opportunities for further enhancement of programmable DNA cleavage by either discovering or engineering an Argonaute variants with exceptionally fast cleavage kinetics at 37°C.

The results presented in this study identify CbAgo/RecB^{exo-}C combination as the most efficient mesophilic DNA-guided DNA-cleaving programmable endonuclease for *in vitro* specific nicking/cleavage of linear dsDNA at otherwise inaccessible locations. The most exciting conclusion of our work is that in the presence of RecB^{exo-}C DNA helicase CbAgo can rapidly bind and cleave targets located as far as 11–12.5 kb away from the end of a linear dsDNA. Furthermore, we have shown that CbAgo and RecB^{exo-}C enzyme combination can cleave targets located close to the end of linear dsDNA and generate DNA fragments with highly specific ssDNA overhangs which are ready for ligation without further enzymatic treatment. We demonstrate that CbAgo-generated DNA fragments can be directionally and seamlessly linked together using a synthetic double-stranded oligonucleotide (Figure 8). With further optimization and improvements, a PCR-free method for seamless DNA assembly may be developed allowing to directionally join long natural DNAs. The information gained from our current work might eventually lead to developing of novel tools for diagnostic and synthetic biology. Our future studies will continue to identify accessory proteins that can aid mesophilic pAgos in cleaving dsDNA *in vitro* and *in vivo*. Furthermore, finding or engineering accessory factors that help Argonautes efficiently and specifically cleave circular dsDNA at physiological temperature may potentially lead to developing tools for genome editing in the future that would be more comparable to CRISPR-Cas mediated genome editing technologies.

DATA AVAILABILITY

Protein and nucleic acid sequences described in this work are publicly available through the databases and accession numbers are indicated within the paper and its Supplementary Tables. All other relevant data are within the main text or described in Supplementary Information.

SUPPLEMENTARY DATA

Supplementary Data are available at NAR Online.

ACKNOWLEDGEMENTS

The authors thank Drs W. Jack, A. Gardner, N. Tanner and E. Hunt for helpful discussions and critical comments on the manuscript; Dr R. Morgan for providing DNA substrate plasmids; Dr P. Hsieh and J.Greci for assistance with RecBCD constructs and purification; L. Mazzola, D. Fuchs, K. Augulewicz and H. Bell for performing core laboratory capillary electrophoresis analysis; J. Curtis and O. Balaisis for technical assistance in preparation of the manuscript and figures.

FUNDING

New England Biolabs, Inc. Funding for open access charge: New England Biolabs, Inc.
Conflict of interest statement. None declared.

REFERENCES

1. Peters,L. and Meister,G. (2007), Argonaute proteins: mediators of RNA silencing. *Mol. Cell.*, **26**, 611–623.
2. Hammond,S.M., Bernstein,E., Beach,D. and Hannon,C.J. (2000) An RNA directed nuclease mediated post-transcriptional gene silencing in Drosophila cells. *Nature*, **404**, 293–296.
3. Hutvagner,G. and Simard,M.J. (2008) Argonaute proteins: key players in RNA silencing. *Nat. Rev. Mol. Cell Biol.*, **9**, 22–32.
4. Ghildiyal,M. and Zamore,P.D. (2009) Small silencing RNAs: an expanding universe. *Nat. Rev. Genet.*, **10**, 94–108.
5. Martinez,J., Patkaniowska,A., Urlaub,H., Luhrmann,R. and Tuschl,T. (2002) Single-stranded antisense siRNAs guide target RNA cleavage in RNAi introduced dsRNA. *Cell*, **110**, 563–574.
6. Hammond,S.M., Bernstein,E., Beach,D. and Hannon,G.J. (2000) An RNA-directed nuclease mediates post-transcriptional gene silencing in drosophila cells. *Nature*, **404**, 293–296.
7. Elbashir,S.M., Harborth,J., Lendeckel,W., Yalcin,A., Weber,K. and Tuschl,T. (2001) Duplexes of 21-nucleotide RNAs mediate RNA interference in mammalian cell culture. *Nature*, **411**, 494–498.
8. Pratt,A.J. and MacRae,I.J. (2009) The RNA-induced silencing complex: a versatile gene-silencing machine. *J. Biol. Chem.*, **284**, 17897–17901.
9. Moazed,D. (2009) Small RNAs in transcriptional gene silencing and genome defense. *Nature*, **457**, 413–420.
10. Makarova,K.S., Wolf,Y.I., van der Oost,J. and V Koonin,E.V. (2009) Prokaryotic homologs of Argonaute proteins are predicted to function as key components of a novel system of defense against mobile genetic elements. *Biol. Direct.*, **4**, 29.
11. Olovnikov,I., Chan,K., Sachidanandam,R., Newman,D. and Aravin,A. (2013) Bacterial argonaute samples the transcriptome to identify foreign DNA. *Mol. Cell*, **51**, 594–605.
12. Swarts,D.C., Makarova,K., Wang,Y., Nakanishi,K., Ketting,R.F., Koonin,E.V., Patel,D.J. and van der Oost,J. (2014) The evolutionary journey of Argonaute proteins. *Nat. Struct. Mol. Biol.*, **21**, 743–753.
13. Hur,J.K., Olovnikov,I. and Aravin,A.A. (2014) Prokaryotic argonautes defend genomes against invasive DNA. *Trends Biochem. Sci.*, **39**, 257–259.
14. Kuzmenko,A., Oguienko,A., Esyunina,D., Yudin,D., Petrova,M., Kudinova,A., Maslova,O., Ninova,M., Ryazansky,S., Leach,D. *et al.* (2020) DNA targeting and interference by a bacterial Argonaute nuclease. *Nature*, **587**, 632–637.
15. Ryazansky,S., Kulbachinskiy,A. and Aravin,A.A. (2018) The expanded universe of prokaryotic Argonaute proteins. *Mbio.*, **9**, e01935-18.
16. Lisitskaya,L., Aravin,A.A. and Kulbahinskiy,A. (2018) DNA interference and beyond: structure and function of prokaryotic Argonaute proteins. *Nat. Commun.*, **9**, 5165.
17. Wang,Y., Juranek,S., Li,H., Sheng,G., Wardle,G.S., Tuschl,T. and Patel,D.J. (2009) Nucleation, propagation and cleavage of target RNAs in argonaute silencing complexes. *Nature*, **461**, 754–761.
18. Sheng,G., Zhao,H., Wang,J., Rao,Y., Tian,W., Swarts,D.C, van der Oost,J., Patel,D.J. and Wang,Y. (2014) Structure-based cleavage mechanism of Thermus thermophilus Argonaute DNA guide strand-mediated DNA target cleavage. *Proc. Natl. Acad. Sci. U.S.A.*, **111**, 652–657.
19. Doxzen,K.W. and Doudna,J.A. (2017) DNA recognition by an RNA-guided bacterial Argonaute. *PLoS One*, **12**, e0177097.
20. Yuan,Y.R, Pei,Y., Ma,J.B., Kuryavyi,V., Zhadina,M., Meister,G., Chen,H.Y., Dauter,Z., Tuschl,T. and Patel,D.J. (2005) Crystal structure of *A. aeolicus* argonaute, a site-specific DNA-guided endoribonuclease, provides insights into RISC-mediated mRNA cleavage. *Mol. Cell.*, **19**, 405–419.
21. Swarts,D.C., Hegge,J.W., Hinojo,I., Shiimori,M., Ellis,M.A., Dumrongkulraksa,J., Terns,R.M., Terns,M.P. and van der Oost,J. (2015) Argonaute of the archaeon Pyrococcus furiosus is a DNA-guided nuclease that targets cognate DNA. *Nucleic Acids Res.*, **43**, 5120–5129.
22. Zander,A., Holzmeister,P., Klose,D., Tinnefeld,P. and Grohmann,D. (2014) Single-molecule FRET supports the two-state model of Argonaute action. *RNA Biol.*, **11**, 45–56.
23. Swarts,D.C., Szczepaniak,M., Sheng,G., Chandradoss,S.D., Zhu,Y., Timmers,E.M., Zhang,Y., Zhao,H., Lou,J., Wang,Y. *et al.* (2017) Autonomous generation and loading of DNA guides by bacterial argonaute. *Mol. Cell.*, **65**, 985–998.
24. Zander,A., Willkomm,S., Ofer,S., van Wolferen,M., Egert,L., Buchmeier,S., Stöckl,S., Tinnefeld,P., Schneider,S., Klingl,A. *et al.* (2017) Guide-independent DNA cleavage by archaeal Argonaute from Methanocaldococcus jannaschii. *Nat. Microbiol.*, **2**, 17034.
25. Kuzmenko,A., Yudin,D., Ryazansky,S., Kulbachinskiy,A. and Aravin,A.A. (2019) Programmable DNA cleavage by ago nucleases from mesophilic bacteria *Clostridium butyricum* and *Limnothrix rosea*. *Nucleic Acids Res.*, **47**, 5822–5836.
26. Swarts,D.C., Jore,M.M., Westra,E.R., Zhu,Y., Janssen,J.H., Snijders,A.P., Wang,Y., Patel,D.J., Berenguer,J., Brouns,S.J.J. *et al.* (2014) DNA-guided DNA interference by a prokaryotic Argonaute. *Nature*, **507**, 258–261.
27. Olina,A., Kuzmenko,A., Ninova,M., Aravin,A.A., Kulbachinskiy,A. and Esyunina.,D. (2020) Genome-wide DNA sampling by ago nuclease from the cyanobacterium *Synechococcus elongatus*. *RNA Biol.*, **17**, 677–688.
28. Kropocheva,E., Kuzmenko,A., Aravin,A.A., Esyunina,D. and Kulbachinskiy,A. (2021) A programmable pAgo nuclease with universal guide and target specificity from mesophilic bacterium *Kurthia massiliensis*. *Nucleic Acids Res.*, **49**, 4054–4065.
29. Hegge,J.W., Swarts,D.C. and van der Oost,J. (2018) Prokaryotic Argonaute proteins: novel genome-editing tools?*Nat. Rev. Microbiol.*, **16**, 5–11.
30. Gasiunas,G., Barrangou,R., Horvath,P. and Siksnys,V. (2012) Cas9–crRNA ribonucleoprotein complex mediates specific DNA cleavage for adaptive immunity in bacteria. *Proc. Natl. Acad. Sci. U.S.A.*, **109**, E2579–E2586.
31. Jinek,M., Chylinski,K., Fonfara,I., Hauer,M., Dudna,J.A. and Charpentier,E. (2012) A programmable dual RNA-guided DNA endonuclease in adaptive bacterial immunity. *Science*, **337**, 816–821.
32. Wang,H., La Russa,M. and Qi,L.S. (2016) CRISPR/Cas9 in genome editing and beyond. *Annu. Rev. Biochem.*, **85**, 227–264.
33. Enghiad,B. and Zhao,H. (2017) Programmable DNA-guided artificial restriction enzymes. ACS synthetic biology. *ACS Synth. Biol.*, **6**, 752–757.

34. Hunt,E.A., Evans,T.C. Jr and Tanner,N.A. (2018) Single-stranded binding proteins and helicase enhance the activity of prokaryotic argonautes in vitro. *PLoS One*, **13**, e0203073.
35. Hegge,J.W., Swarts,D.C., Chandradoss,S.D., Cui,T.J., Kneppers,J., Jinek,M., Joo,C. and van der Oost,J. (2019) DNA-guided DNA cleavage at moderate temperatures by Clostridium butyricum Argonaute. *Nucleic Acids Res.*, **47**, 5809–5821.
36. Cao,Y., Sun,W., Wang,J., Sheng,G., Xiang,G., Zhang,T., Shi,W., Li,C., Wang,Y., Zhao,F. *et al.* (2019) Argonaute proteins from human gastrointestinal bacteria catalyze DNA-guided cleavage of single- and double-stranded DNA at 37°C. *Cell Discov.*, **5**, 38.
37. Liu,Y., Li,W., Jiang,X., Wang,Y., Zhang,Z., Liu,Q., He,R., Chen,Q., Yang,J., Wang,L. *et al.* (2021) A programmable omnipotent Argonaute nuclease from mesophilic bacteria *Kurthia massiliensis*. *Nucleic Acids Res.*, **49**, 1597–1608.
38. Willkomm,S., Zander,A., Gust,A. and Grohmann,D.A (2015) Prokaryotic twist on argonaute function. *Life*, **5**, 538–553.
39. Raney,K.D., Byrd,A.K. and Aarattuthodiyil,S. (2013) Structure and mechanism of SF1 DNA helicases. *Adv. Exp. Med. Biol.*, **767**, 17–46.
40. Taylor,A.F. and Smith,G.R. (1985) Substrate specificity of the DNA unwinding activity of the RecBC enzyme of Escherichia coli. *J. Mol. Biol.*, **185**, 431–443.
41. Taylor,A. and Smith,G.R. (1980) Unwinding and rewinding of DNA by the RecBC enzyme. *Cell*, **22**, 447–457.
42. Dillingham,M.C. and Kowalczykowski,S.C. (2008) RecBCD enzyme and the repair of double-stranded DNA breaks. *Microbiol. Mol. Biol. Rev.*, **72**, 642–671.
43. Masterson,C., Boehmer,P.E., McDonald,F., Chaudhuri,S., Hickson,I.D. and Emmerson,P.T. (1992) Reconstitution of the activities of the RecBCD holoenzyme of Escherichia coli from the purified subunits. *J. Biol. Chem.*, **267**, 13564–13572.
44. Yu,M., Souaya,J. and Julin,D.A. (1992) The 30-kDa C-terminal domain of the RecB protein is critical for the nuclease activity, but not the helicase activity, of the RecBCD enzyme from Escherichia coli. *Proc. Natl. Acad. Sci. U.S.A.*, **95**, 981–986.
45. Sun,J.Z., Julin,D.A. and Hu,J.S. (2006) The nuclease domain of the Escherichia coli RecBCD enzyme catalyzes degradation of linear and circular single-stranded and double-stranded DNA. *Biochemistry*, **45**, 131–140.
46. Wang,J., Chen,R. and Julin,D.A. (2000) A single nuclease active site of the *Escherichia coli* RecBCD enzyme catalyzes single-stranded DNA degradation in both directions. *J. Biol. Chem.*, **275**, 507–513.
47. Singleton,M.R., Dillingham,M.S., Gaudier,M., Kowalczykowski,S.C. and Wigley,D.B. (2004) Crystal structure of RecBCD enzyme reveals a machine for processing DNA breaks. *Nature*, **432**, 187–193.
48. Korangy,F. and Julin,D.A. (1992) A mutation in the consensus ATP-binding sequence of the RecD subunit reduces the processivitybof the RecBCD enzyme from *Escherichia coli*. *J. Biol. Chem.*, **267**, 3088–3095.
49. Korangy,F. and Julin,D.A. (1993) Kinetics and processivity of ATP hydrolysis and DNA unwinding by the RecBC enzyme from *Escherichia coli*. *Biochemistry*, **32**, 4873–4880.
50. Korangy,F. and Julin,D.A. (1994) Efficiency of ATP hydrolysis and DNA unwinding by the RecBC enzyme from from *Escherichia coli*. *Biochemistry*, **33**, 9552–9560.
51. Garcia-Quintans,N., Bowden,L., Berenguer,J. and Mencia,M. (2020) DNA interference by mesophilic argonaute CbcAgo. *F1000 Research*, **8**, e321.
52. Greenough,L., Schermerhorn,K.M., Mazzola,L., Bybee,J., Rivizzigno,D., Cantin,E., Slatko,B.E. and Gardner,A.F. (2016) Adapting capillary gel electrophoresis as a sensitive, high-throughput method to accelerate characterization of nucleic acid metabolic enzymes. *Nucleic Acids Res.*, **44**, e15.
53. Edgar,R.C. (2004) MUSCLE: multiple sequence alignment with high accuracy and high throughput. *Nucleic Acids Res.*, **32**, 1792–1797.
54. Eddy,S.R. (2011) Accelerated profile HMM searches. *PLoS Comp. Biol.*, **7**, e1002195.
55. Gerritsen,J., Fuentes,S., Grievink,W., van Niftrik,L., Tindall,B.J., Timmerman,H.M., Rijkers,G.T. and Smidt,H. (2014) Characterization of *Romboutsia ilealis* gen. nov., sp. nov., isolated from the gastro-intestinal tract of a rat, and proposal for the reclassification of five closely related members of the genus *Clostridium* into the genera *Romboutsia* gen. nov., *Intestinibacter* gen. nov., *Terrisporobacter* gen. nov. and *Asaccharospora* gen. nov. *J. Syst. Evol. Microbiol.*, **64**, 1600–1616.
56. Umezu,K., Nakayama,K. and Nakayama,H. (1990) *Escherichia coli* RecQ protein is a DNA helicase. *Proc. Natl. Acad. Sci. U.S.A.*, **87**, 5363–5367.
57. Umezu,K. and Nakayama,H. (1993) RecQ DNA helicase of Escherichia coli. Characterization of the helix-unwinding activity with emphasis on the effect of single-stranded DNA-binding protein., *J. Mol. Biol.*, **230**, 1145–1150.
58. Rad,B., Forget,A.L., Baskin,R.J. and Kowalczykowski,S.C. (2015) Single-molecule visualization of RecQ helicase reveals DNA melting, nucleation, and assembly are required for processive DNA unwinding. *Proc. Natl. Acad. Sci. U.S.A.*, **112**, E6852–E6861.
59. Hunt,E.A., Tamanaha,E., Bonanno,K., Cantor,E.J. and Tanner,N.A. (2021) Profiling *Thermus thermophilus* Argonaute guide DNA sequence preference by functional screening. *Front. Mol. Biosci.*, **8**, 670940.
60. Willkomm,S., Oellig,C.A., Zander,A., Restle,T., Keegan,R., Grohmann,D. and Schneider,S. (2017) Structural and mechanistic insights into an archaeal DNA-guided Argonaute protein. *Nat. Microbiol.*, **2**, 17035.
61. Wang,Y., sheng,G., Juratnek,T., Tuschl,T. and Patel,D.J. (2008) Structure of the guide-strand-containing argonaute silencing complex. *Nature*, **456**, 209–213.